D^- mesic atoms

C. García-Recio

Departamento de Física Atómica Molecular y Nuclear, and

Instituto Carlos I de Física Teórica y Computacional, Universidad de Granada, E-18071 Granada, Spain

J. Nieves

Instituto de Física Corpuscular (IFIC), Centro Mixto CSIC-Universidad de Valencia

Institutos de Investigación de Paterna, Aptd. 22085, E-46071 Valencia, Spain

L. L. Salcedo

Departamento de Física Atómica Molecular y Nuclear, and

Instituto Carlos I de Física Teórica y Computacional, Universidad de Granada, E-18071 Granada, Spain

L. Tolos

Institut de Ciències de l'Espai (IEEC/CSIC), Campus Universitat Autònoma de Barcelona,

Facultat de Ciències, Torre C5, E-08193 Bellaterra, Spain

November 29, 2011

Abstract

The anti-D meson self-energy is evaluated self-consistently, using unitarized coupled-channel theory, by computing the in-medium meson-baryon T-matrix in the $C = -1, S = 0$ sector. The heavy pseudo-scalar and heavy vector mesons, $\bar{D}$ and $\bar{D}^*$, are treated on equal footing as required by heavy quark spin symmetry. Results for energy levels and widths of D^- mesic atoms in ^{12}C, ^{40}Ca, ^{118}Sn and ^{208}Pb are presented. The spectrum contains states of atomic and of nuclear types for all nuclei. $\bar{D}^0$-nucleus bound states are also obtained. We find that, after electromagnetic and nuclear cascade, these systems end up with the $\bar{D}$ bound in the nucleus, either as a meson or as part of a exotic $\bar{D}N$ (pentaquark) loosely bound state.

1 Introduction

Hadronic atoms provide valuable information about in-medium modification of hadron properties, on hadron-nucleon interaction, and also on properties of nuclei not easily accessible by other probes, as the distribution density of neutrons. This field has been the subject of thorough study, both theoretical and experimental, since long time ago for pions and anti-kaons [1, 2, 3, 4, 5, 6], and more recently for anti-protons [7, 8, 9]. However, for anti-charmed atoms not much theoretical work exists in the literature. To our knowledge, only Ref. [10] studies D^- atoms. There, the $1s$, $2s$ and $1p$ states (neglecting widths) of D^- in ^{208}Pb were evaluated using the quark-meson coupling model of Ref. [11]. $\bar{D}NN$ bound states (rather than atoms) were predicted in [12]. On

the experimental side, the study of anti-D mesic atoms poses a serious challenge. The study of open charm systems seems timely in view of the forthcoming experiments by the PANDA [13, 14] and CBM [15, 16] Collaborations at the future FAIR facility at Darmstadt [17].

As compared to other mesic atoms, D^- atoms have a number of specific features that make them worth studying. First, the $\bar{D}$ meson is so heavy that the atomic meson wave function has a sizable overlap with the nucleus, specially for the low lying levels and for heavy nuclei. Hence the strong interaction effects are expected to be larger than for other mesic atoms, even if the optical potentials themselves are of comparable strength. Second, $\bar{D}N$ has no lower hadronic channels for strong interaction decay. This is unlike other hadron-nucleus bound systems. For instance, in pionic atoms the channel $\pi NN \to NN$ is available, in K^- atoms $\bar{K}N \to \pi\Lambda$ and $\pi\Sigma$, in D^0-nucleus $DN \to \pi\Lambda_c$ and $\pi\Sigma_c$, in $\bar{p}$ atoms $\bar{p}N \to$pions, or in η-nucleus, $\eta N \to \pi N$. So, if bound, the $\bar{D}$ remains in the nucleus until its weak decay is produced. Third, heavy quark spin symmetry (HQSS), a well established approximate QCD symmetry [18, 19], is expected to play an important role in D^- atoms. One of the consequences of HQSS is that the $\bar{D}^*$ vector meson degrees of freedom should have some (important) influence on these systems. Hence, such degrees of freedom should be incorporated by means of any realistic treatment. This is automatically achieved in the SU(8) extended Weinberg-Tomozawa model followed in this work [20, 21]. Fourth, all t-channel vector meson exchange models without incorporating HQSS, that is, not including vector mesons in the coupled-channel space, produce a featureless real repulsive potential below threshold [22, 23, 24]. This scenario is expected to change when HQSS is enforced. Indeed, the calculation of [12] identifies an $I = 0, J = 1/2^-$ $\bar{D}N$ bound state with $1.4\,\mathrm{MeV}$ of binding energy. The same state is also found in the SU(8) model of Ref. [21]. This exotic baryonic state plays an important role in the D^- atom dynamics. Due to the existence of this exotic state, the $\bar{D}$ optical potential turns out to be attractive, dissipative and strongly energy dependent. In addition, due to the energy dependence, not so relevant in other mesic atoms, a proper implementation of the electromagnetic interaction, through minimal coupling, needs to be considered.

The paper is organized as follows. In Sect. 2 we describe the calculation of the $\bar{D}$ self-energy in nuclear matter and present our results for the $\bar{D}$ optical potential. We carry out a self-consistent calculation in symmetric nuclear matter at zero temperature for energies around the $\bar{D}$ mass. In Sect. 3 we present our results for the energies and widths of the D^- mesic atom levels in ^{12}C, ^{40}Ca, ^{118}Sn and ^{208}Pb. For this purpose, we solve the Schrödinger equation with a finite nuclei $\bar{D}$ optical potential obtained from that derived for nuclear matter, in the previous section, and making use of the local density approximation. In this section, we also extend our study to the case of $\bar{D}^0$ bound states. Finally in Sect. 4, we discuss possible decay mechanisms of the bound states, while in Sect. 5 we summarize the main conclusions of the present work.

2 The $\bar{D}$ self-energy and optical potential

The self-energy in symmetric nuclear matter for the $\bar{D}$ meson is obtained following a self-consistent procedure in coupled channels, as similarly done for the D meson [25]. The s-wave transition potential of the Bethe-Salpeter equation is derived from an effective Lagrangian that implements HQSS. This is an approximate QCD symmetry that treats on equal footing heavy pseudo-scalar and vector mesons [18, 19]. Therefore, we calculate simultaneously the self-energy of the $\bar{D}^*$, the HQSS partner of the $\bar{D}$.

As shown in [26, 27], the Weinberg-Tomozawa (WT) meson-baryon Lagrangian admits a unique and natural extension with spin-flavor symmetry for any number of flavors. In addition to 0^+ mesons and $1/2^+$ baryons, this requires the inclusion of 1^- mesons and $3/2^+$ baryons. For four flavors this interaction has SU(8) symmetry and automatically enjoys HQSS in the $C = -1$ sector. Schematically [20, 21],

$$\mathcal{L}_{\mathrm{WT}}^{\mathrm{SU(8)}} = \frac{1}{f^2} \left((M^\dagger \otimes M)_{\mathbf{63}_a} \otimes (B^\dagger \otimes B)_{\mathbf{63}} \right)_{\mathbf{1}}. \tag{1}$$

The tree level amplitudes for different isospin (I), total angular momentum (J), charm (C) and strangeness (S) take the form

$$V_{ab}^{IJSC}(\sqrt{s}) = D_{ab}^{IJSC} \frac{2\sqrt{s} - M_a - M_b}{4\, f_a f_b} \sqrt{\frac{E_a + M_a}{2M_a}} \sqrt{\frac{E_b + M_b}{2M_b}}, \tag{2}$$

where M_a (M_b) and E_a (E_b) are, respectively, the mass and the center of mass energy of the baryon in the a (b) channel. The matrix elements D_{ab}^{IJSC} of the SU(8) WT interaction can be obtained from Wick contractions using the hadronic wave functions [20] or by means of the SU(8)⊃SU(4)⊗SU(2) Clebsch-Gordan coefficients [28]. The spin-flavor SU(8) symmetry is strongly broken in nature and this is incorporated by adopting the physical hadron masses and different weak decay constants, f_a, for non-charmed and charmed, pseudo-scalar and vector mesons [20, 21].

In what follows, we focus in the non-strange $(S = 0)$ and singly anti-charmed $(C = -1)$ sector, where the $\bar{D}N$ and $\bar{D}^*N$ states are embedded. The channels involved in the coupled-channel calculation are: $\bar{D}N$ and $\bar{D}^*N$ for $I = 0, J = 1/2$; $\bar{D}^*N$ for $I = 0, J = 3/2$; $\bar{D}N$, $\bar{D}^*N$ and $\bar{D}^*\Delta$ for $I = 1, J = 1/2$; and $\bar{D}\Delta$, $\bar{D}^*N$ and $\bar{D}^*\Delta$ for $I = 1, J = 3/2$.

The amplitudes in nuclear matter $[T^{\rho,IJ}(P_0, \boldsymbol{P})]$ are obtained by solving the on-shell Bethe-Salpeter equation with the tree level amplitude $V^{IJ}(\sqrt{s})$:

$$T^{\rho,IJ}(P) = \frac{1}{1 - V^{IJ}(\sqrt{s})\, G^{\rho,IJ}(P)} V^{IJ}(\sqrt{s}), \tag{3}$$

where the diagonal $G^{\rho,IJ}(P)$ matrix accounts for the meson-baryon loop in nuclear matter. The logarithmic divergence in the vacuum part of the loop function, $G^0(\sqrt{s})$, is removed by subtraction. Following [20, 21], we set $G^{0,IJ}(\sqrt{s} = \mu^{IJ}) = 0$ with

$$\left(\mu^{IJ}\right)^2 = \alpha \left(m_{\mathrm{th}}^2 + M_{\mathrm{th}}^2\right). \tag{4}$$

Here m_{th} and M_{th} are, respectively, the meson and baryon masses of the hadronic channel with lowest mass threshold for the given I, J. The value of the parameter α is set to one [29]. However, in the following, we will also vary α to have an estimate of the sensitivity of our results against changes in the regularization scale.

Nuclear matter effects enter in the meson-baryon loop function $G^{\rho,IJ}(P)$. One of the sources of density dependence comes from Pauli blocking. Another source is related to the change of the properties of mesons and baryons in the intermediate states due to the interaction with nucleons of the Fermi sea. We proceed as in Ref. [25], where the most important changes in matter came from the Pauli blocking of nucleons and from the self-consistent treatment of the open charm self-energies.

3

Thus, for the $\bar{D}N$ and $\bar{D}^*N$ channels, the meson-baryon loop function in matter is given by [25]:

$$
\begin{aligned}
G^{\rho}_{\bar{D}(\bar{D}^*)N}(P) \;=\; & G^0_{\bar{D}(\bar{D}^*)N}(\sqrt{s}) + \int \frac{d^3q}{(2\pi)^3}\frac{M_N}{E_N(\boldsymbol{p})}\left[\frac{-n(\boldsymbol{p})}{(P^0 - E_N(\boldsymbol{p}))^2 - \omega(\boldsymbol{q})^2 + i\varepsilon} \right. \\
& \left. +(1-n(\boldsymbol{p}))\left(\frac{-1/(2\omega(\boldsymbol{q}))}{P^0 - E_N(\boldsymbol{p}) - \omega(\boldsymbol{q}) + i\varepsilon} + \int_0^\infty d\omega \frac{S_{\bar{D}(\bar{D}^*)}(\omega,\boldsymbol{q})}{P^0 - E_N(\boldsymbol{p}) - \omega + i\varepsilon}\right)\right]\Bigg|_{\boldsymbol{p}=\boldsymbol{P}-\boldsymbol{q}},
\end{aligned}
\tag{5}
$$

where $E_N(\boldsymbol{p}) = \sqrt{\boldsymbol{p}^2 + M_N^2}$ is the nucleon energy and $\omega(\boldsymbol{q}) = \sqrt{\boldsymbol{q}^2 + m^2_{\bar{D}(\bar{D}^*)}}$ is the $\bar{D}(\bar{D}^*)$ energy. The free loop function $G^0(\sqrt{s})$ is corrected in matter by terms proportional to the nucleon Fermi distribution $n(\boldsymbol{p}) = \Theta(|\boldsymbol{p}|-p_F)$ that takes into account Pauli blocking effects. The quantities $\boldsymbol{p}$ and p_F are the momentum of the nucleon and the Fermi momentum at nuclear density ρ, respectively. The implementation of the $\bar{D}$ and $\bar{D}^*$ properties in matter comes through the meson spectral functions, $S_{\bar{D}(\bar{D}^*)}(\omega,\boldsymbol{q})$, which are defined from the in-medium $\bar{D}$ and $\bar{D}^*$ meson propagators:

$$
\begin{aligned}
D^{\rho}_{\bar{D}(\bar{D}^*)}(q) \;&=\; \left((q^0)^2 - \omega(\boldsymbol{q})^2 - \Pi_{\bar{D}(\bar{D}^*)}(q)\right)^{-1}, \\
S_{\bar{D}(\bar{D}^*)}(q) \;&=\; -\frac{1}{\pi}\,\mathrm{Im}D^{\rho}_{\bar{D}(\bar{D}^*)}(q) \quad (\text{for } q^0 > 0).
\end{aligned}
\tag{6}
$$

The self-energies, $\Pi_{\bar{D}(\bar{D}^*)}(q^0,\boldsymbol{q};\rho)$, are obtained self-consistently from the in-medium $\bar{D}N$ and $\bar{D}^*N$ effective interactions as we will show in the following. As for $\bar{D}\Delta$ and $\bar{D}^*\Delta$ channels, we include the self-energy of the $\bar{D}$ and $\bar{D}^*$ mesons. Then, the equivalent of Eq. (5) for those channels reads [25]

$$
\begin{aligned}
G^{\rho}_{\bar{D}(\bar{D}^*)\Delta}(P) \;=\; & G^0_{\bar{D}(\bar{D}^*)\Delta}(\sqrt{s}) + \int \frac{d^3q}{(2\pi)^3}\frac{M_\Delta}{E_\Delta(\boldsymbol{p})}\left(\frac{-1/(2\omega(\boldsymbol{q}))}{P^0 - E_\Delta(\boldsymbol{p}) - \omega(\boldsymbol{q}) + i\varepsilon}\right. \\
& \left. + \int_0^\infty d\omega \frac{S_{\bar{D}(\bar{D}^*)}(\omega,\boldsymbol{q})}{P^0 - E_\Delta(\boldsymbol{p}) - \omega + i\varepsilon}\right)\Bigg|_{\boldsymbol{p}=\boldsymbol{P}-\boldsymbol{q}},
\end{aligned}
\tag{7}
$$

with $E_\Delta(\boldsymbol{p}) = \sqrt{\boldsymbol{p}^2 + M_\Delta^2}$. The effect of the vacuum width of the Δ has not been included. The strong width of the $\bar{D}^*$ is very small, as a consequence of HQSS.

The $\bar{D}$ self-energy in symmetric nuclear matter is obtained by summing the different isospin transition amplitudes for $\bar{D}N$ over the nucleon Fermi distribution as

$$
\Pi_{\bar{D}}(q^0,\boldsymbol{q};\rho) \;=\; \int_{p\leq p_F} \frac{d^3p}{(2\pi)^3}\left[T^{\rho,0,1/2}_{\bar{D}N}(P^0,\boldsymbol{P}) + 3\,T^{\rho,1,1/2}_{\bar{D}N}(P^0,\boldsymbol{P})\right].
\tag{8}
$$

Simultaneously, the $\bar{D}^*$ meson self-energy is derived from the sum over the $\bar{D}^*N$ amplitudes as[1]

$$
\begin{aligned}
\Pi_{\bar{D}^*}(q^0,\boldsymbol{q};\rho) \;=\; & \int_{p\leq p_F} \frac{d^3p}{(2\pi)^3}\left[\frac{1}{3}\,T^{\rho,0,1/2}_{\bar{D}^*N}(P^0,\boldsymbol{P}) + T^{\rho,1,1/2}_{\bar{D}^*N}(P^0,\boldsymbol{P})\right. \\
& \left. +\frac{2}{3}\,T^{\rho,0,3/2}_{\bar{D}^*N}(P^0,\boldsymbol{P}) + 2\,T^{\rho,1,3/2}_{\bar{D}^*N}(P^0,\boldsymbol{P})\right].
\end{aligned}
\tag{9}
$$

---

[1] We neglect the enhancement in the $\bar{D}^*$ width due to coupling to $\bar{D}\pi$ (and their medium corrections). The analogous mechanism for $\bar{K}^* \to \bar{K}\pi$ was considered in [30].
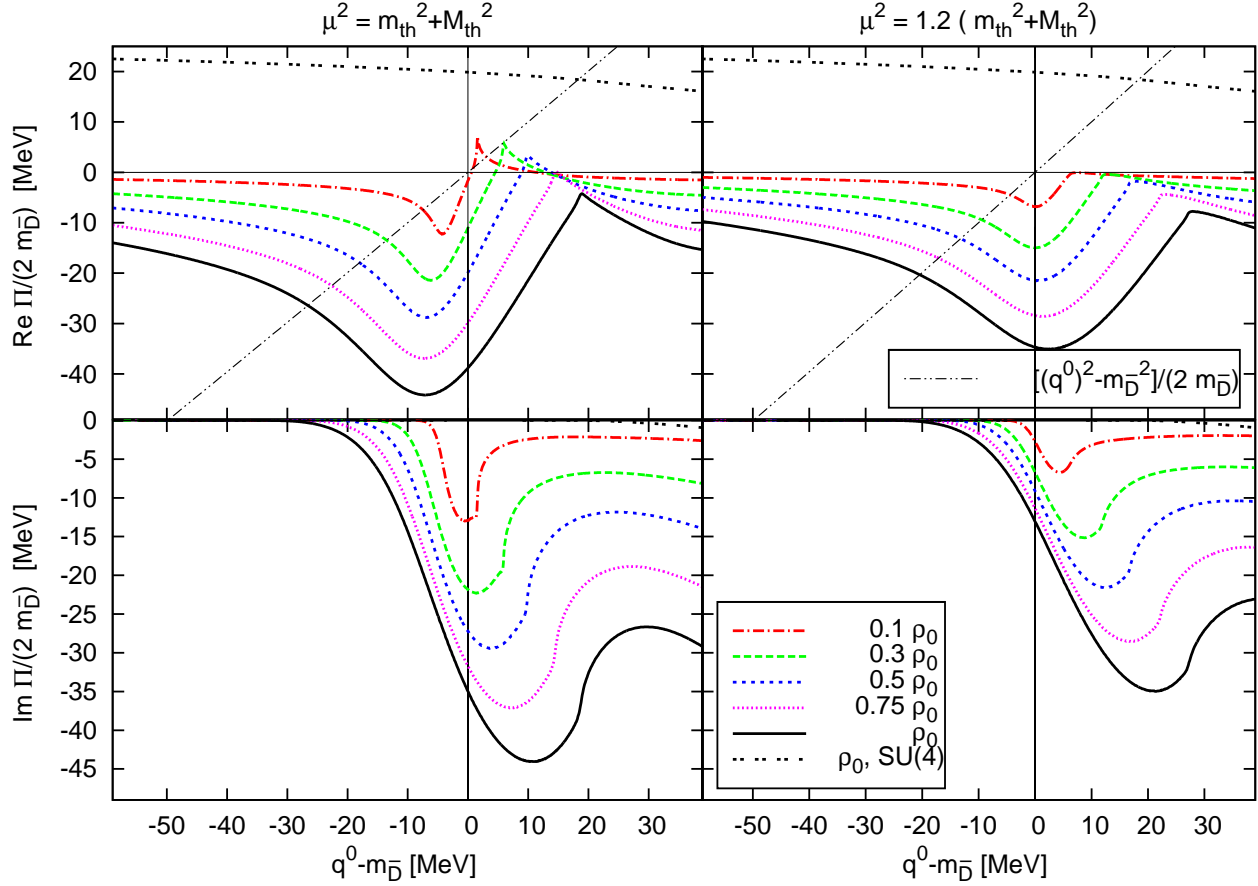
Figure 1: Real and imaginary parts of the $\bar{D}$ self-energy over $2m_{\bar{D}}$, at $\boldsymbol{q} = 0$, as functions of the meson energy q^0 for different densities and two subtraction points with $\alpha = 1$ (left panels) and $\alpha = 1.2$ (right panels). The oblique line is the function $((q^0)^2 - m_{\bar{D}}^2)/(2m_{\bar{D}})$. The SU(4) $\bar{D}$ self-energy obtained in Ref. [23] for normal nuclear matter density is also displayed.

In the above equations, $P^0 = q^0 + E_N(\boldsymbol{p})$ and $\boldsymbol{P} = \boldsymbol{q} + \boldsymbol{p}$ are the total energy and momentum of the meson-nucleon pair in the nuclear matter rest frame, and $(q^0, \boldsymbol{q})$ and $(E_N, \boldsymbol{p})$ stand for the energy and momentum of the meson and nucleon, respectively, in that frame. As mentioned previously, those self-energies are determined self-consistently since they are obtained from the in-medium amplitudes which contain the meson-baryon loop functions, and those quantities themselves are functions of the self-energies.

We are interested in studying possible $\bar{D}$ bound states in nuclei. Therefore, we concentrate on the self-energy for q^0 around the $\bar{D}$ mass. In Fig. 1 we show the $\bar{D}$ self-energy over $2m_{\bar{D}}$, as a function of the $\bar{D}$ energy, for various nuclear densities ρ, and with the $\bar{D}$ meson momentum $\boldsymbol{q} = 0$. We display results for two values for the subtraction point (see Eq. (4)): $\alpha = 1$ (left panels) and $\alpha = 1.2$ (right panels). For comparison, we also show results for the SU(4) WT model of Ref. [23] at normal nuclear density, $\rho_0 = 0.17$ fm^{-3}.

It is worth noticing a resonant structure (more pronounced for the preferred value $\alpha = 1$) close to the $\bar{D}N$ threshold, which will be of up-most importance for the study of $\bar{D}$ bound states. This

structure results from a pole in the free space amplitude of the sector $I = 0, J = 1/2$ at $2805\,\text{MeV}$ (a weakly bound pentaquark state) that strongly couples to $\bar{D}N$ and $\bar{D}^*N$ states [21] (also found in [12]). For reference we will call this state $X(2805)^2$. The situation has some similarities with the $\bar{K}N$ interaction, which is governed by the $\Lambda(1405)$ resonance. The $\Lambda(1405)$ dominates the behavior of the $\bar{K}N$ interaction close to threshold similarly to the pole in $2805\,\text{MeV}$ for the $\bar{D}N$ amplitude. However, the $\Lambda(1405)$ can decay into $\pi\Sigma$, whereas the $X(2805)$ is below all thresholds for strong interaction decay. The exotic $X(2805)$ has a HQSS partner with $I = 0, J = 3/2$, a $\bar{D}^*N$ bound state with mass $2922\,\text{MeV}$, as seen in Ref. [21].

In contrast to the SU(8) scheme and as mentioned above, a resonant structure is not observed in the SU(4) WT model of Ref. [23]. The SU(4) amplitude is repulsive and shows a smooth behavior as a function of the energy. A similar repulsive effect was observed in the t-channel vector meson exchange models of Refs. [22, 24].

Due to the strong energy dependence of the in-medium effective interaction in the SU(8) WT scheme close to threshold, any slight change in the parameters of the model as well as in the self-consistent procedure may have strong consequences on the formation of $\bar{D}$-nucleus bound states. In order to mimic those changes, we have slightly varied the subtraction point, namely, to $\alpha = 1.2$. In this way we study two very distinct situations for the formation of bound states and set our theoretical uncertainties.

The $\bar{D}$ self-energy is evaluated in infinite nuclear matter. In finite nuclei we use the local density approximation (LDA), substituting ρ by $\rho(r)$, which is the local density at each point in the nucleus. For the s-wave, as it is the case here, it was shown in Ref. [3] that the LDA gave the same results as a direct finite nucleus calculation. The LDA $\bar{D}$ self-energy allows to define a local optical potential. In mesic atoms this optical potential is often taken to be energy independent and fixed to its value at threshold ($q^0 = m_{\bar{D}}$, $\boldsymbol{q} = 0$). However, both the real and the imaginary parts of the $\bar{D}$ self-energy, around the $\bar{D}$-meson mass, show a pronounced energy dependence, as can be appreciated in Fig. 1. Hence, a realistic determination of the $\bar{D}$ bound states should take this energy dependence into account, as done previously for η- and D^0-nucleus systems [31, 32]. Thus, we use an energy dependent optical potential defined as:

$$V_{\text{opt}}(r, q^0) = \frac{1}{2q^0}\Pi_{\bar{D}}(q^0, \boldsymbol{q} = 0, \rho(r)). \tag{10}$$

Most of the imaginary part for $q^0 < m_{\bar{D}}$ displayed in Fig. 1 comes from particle-hole production and this is allowed due to the attractive potential felt by the $\bar{D}$ in the medium. The quantity $((q^0)^2 - m_{\bar{D}}^2)/(2m_{\bar{D}})$ is displayed in Fig. 1 by a dashed-dotted-dotted solid line. The leftmost crossing point of this line with the real part of the self-energy (divided by $2m_{\bar{D}}$) signals the opening of the $\bar{D}$-particle-hole threshold. For the energies displayed, $((q^0)^2 - m_{\bar{D}}^2)/(2m_{\bar{D}})$ is essentially $q^0 - m_{\bar{D}} = E$, the non relativistic energy of the $\bar{D}$ (and so almost a straight line). Therefore, the difference $E - \text{Re}\,V_{\text{opt}}(E)$ corresponds to the kinetic energy of the non-relativistic problem. The two lines E and $\text{Re}\,V_{\text{opt}}(E)$ cross at the classical turning point. Roughly speaking, there should not be imaginary part in the classically forbidden region $E < \text{Re}\,V_{\text{opt}}(E)$, as there is no available

---

^{2}This state is bound by only about 1 MeV in the free space, and it is one of the most interesting predictions of Ref. [21]. Moreover, it appears as a consequence of considering heavy vector meson degrees of freedom, as required by HQSS. Indeed, the diagonal $\bar{D}N$ WT interaction is zero in this sector and thus, the $X(2805)$ is generated thanks to the coupled channel dynamics between the $\bar{D}N$ and $\bar{D}^*N$ pairs. Thus, this bound state is absent in the free space SU(4) WT model of Ref. [29] in which is based the nuclear medium approach of Ref. [23].

phase space for decay (i.e., no kinetic energy to expend). Also, the bound states should appear predominantly for energies fulfilling the condition $E > \mathrm{Re}\, V_{\mathrm{opt}}(E)$, since the expectation value of the kinetic energy in the bound state cannot be negative. Of course, these arguments are only qualitative because the optical potential is complex and strongly energy dependent. This allows for the $\bar{D}$ in the medium to have some non intuitive behavior. For instance, a $\bar{D}$ with energy E can eject a particle-hole going to a lower energy E', and yet end up with more kinetic energy to expend, provided $E - E' < \mathrm{Re}\, V_{\mathrm{opt}}(E) - \mathrm{Re}\, V_{\mathrm{opt}}(E')$.

Due to the $\bar{D}N$ bound state close to threshold, $X(2805)$, the low density approximation $T\rho$ breaks down very early. For a given value of the energy the density dependence of the optical potential is far from linear. For subsequent use, we have computed the optical potential for several densities (those in Fig. 1) and a fine lattice of energies, and have used an interpolation procedure for other values of density and energy. The presence of the bound state/resonance prevented the self-consistent procedure to be continued for densities below $0.1\,\rho_0$.

3   Results

We look first for D^--nucleus bound states by solving the Schrödinger equation:

$$\left[-\frac{\boldsymbol{\nabla}^2}{2m_{\mathrm{red}}} + V_{\mathrm{coul}}(r) + V_{\mathrm{opt}}(r) \right] \Psi = (-B - i\Gamma/2)\Psi. \tag{11}$$

In this equation, B is the binding energy ($B > 0$), Γ the width of the bound state and m_{red} is the $\bar{D}$-nucleus reduced mass. $V_{\mathrm{coul}}(r)$ is the Coulomb potential of the D^- including the nucleus finite size and the Uehling vacuum polarization. $V_{\mathrm{opt}}(r)$ is the energy dependent optical potential. Because the electromagnetic interaction is introduced by means of the minimal coupling prescription (to be consistent with gauge invariance and electric charge conservation), $V_{\mathrm{coul}}(r)$ must be introduced wherever the energy is present. So the energy dependent optical potential of Eq. (10) is applied with argument $q^0 = m_{\bar{D}} - B - V_{\mathrm{coul}}(r)$.

The non relativistic approximation is used since the $\bar{D}$-meson optical potential is much smaller than its mass, and we expect the relativistic corrections to be tiny and certainly smaller than the theoretical uncertainties of the interaction. In the same approximation the denominator $2q^0$ in Eq. (10) can also be set to $2m_{\bar{D}}$.

We solve the Schrödinger equation in coordinate space by using a numerical algorithm [33, 34], which has been extensively tested in similar problems of pionic [3, 4] and anti-kaonic [35, 36] atomic states, in the search of possible anti-kaon [35], η [31], ϕ [37], and D^0 [32] nuclear bound states. Charge densities are taken from Refs. [38, 39]. For each nucleus, we take the neutron matter density approximately equal to the charge one, though we consider small changes, inspired by Hartree-Fock calculations with the density-matrix expansion [40] and corroborated by pionic atom analysis [4]. All the densities used throughout this work can be found in Table 1 of Ref. [35]. The correction in the nuclear density to remove the finite size of the nucleon is introduced following the scheme of Refs. [41][3] and [4]. We have also considered that in nuclei it is necessary a finite energy, of the order of few MeV's, to extract a nucleon. However, in nuclear matter this is not the case and particle-hole excitations can be produced at zero energy transfer. To improve on this deficiency, we have included in our calculation an average energy-gap in the nucleon spectrum. It

---

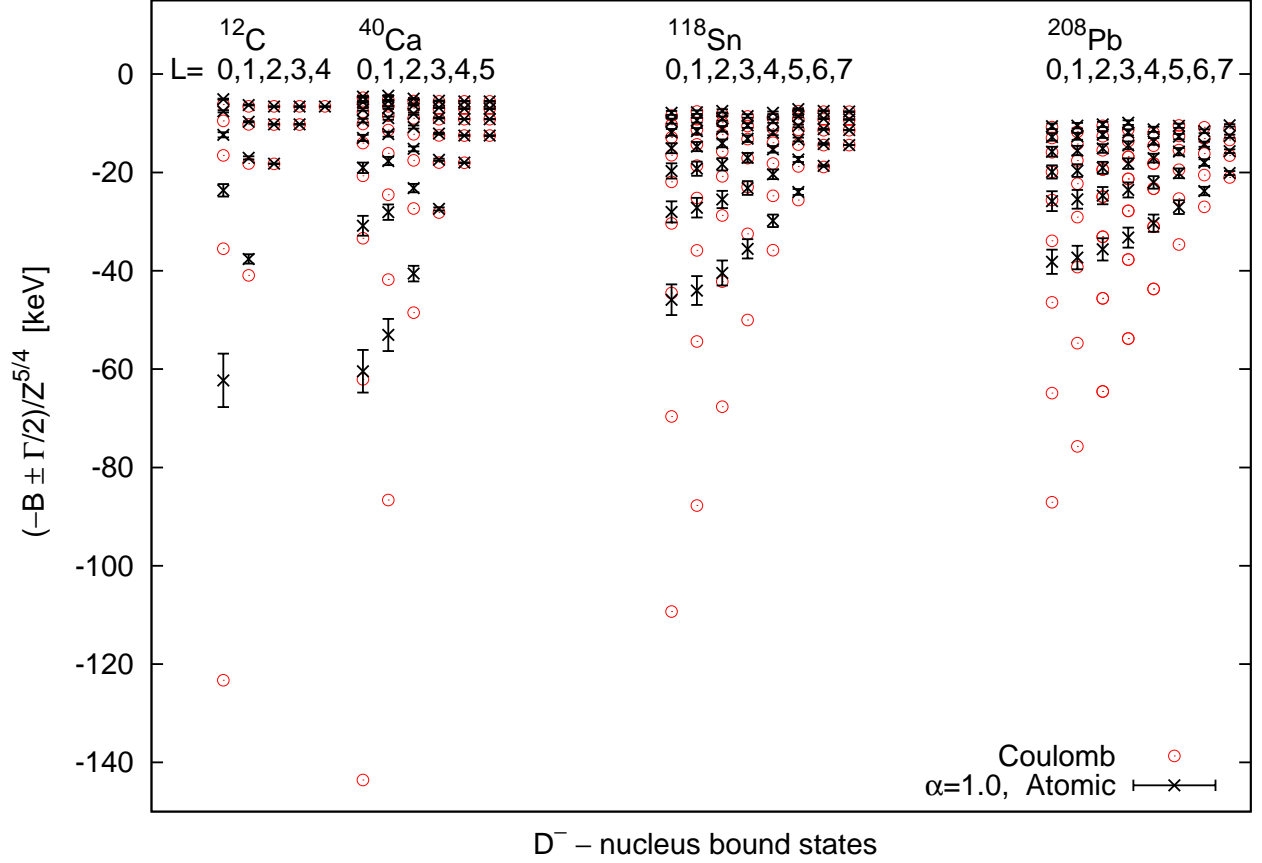[3]πR^2 in Eq. (6.13) of [41] should be corrected to $\pi^2 R$.

Figure 2: D^- atom levels for different nuclei and angular momenta. "⊙" points stand for pure Coulomb potential binding energies (Table 1), while "×" symbols stand for the binding energies and widths of atomic levels predicted by the SU(8) model derived in this work (see Fig. 1), with $\alpha = 1$ and gap $8\,\mathrm{MeV}$ (Table 2). The results are scaled down by a factor $Z^{5/4}$.

is used to shift the imaginary part of the optical potential, thereby reducing the available phase space for extracting a nucleon from the Fermi sea.

In Tables 1–5, we present results for ^{12}C, ^{40}Ca, ^{118}Sn and ^{208}Pb and for several interactions. We have considered:

i) only Coulomb interaction, neglecting totally the nuclear optical potential (Table 1).

ii) Coulomb interaction plus the SU(8) optical potential of Fig. 1, with $\alpha = 1$ (α is defined in Eq. (4)) and a gap in the nucleon spectrum of $8\,\mathrm{MeV}$ (Table 2).

iii) only the SU(8) optical potential with $\alpha = 1$ and a gap of 8 MeV, thus neglecting in this case the Coulomb interaction (Table 3). This applies to $\bar{D}^0$-nucleus states.

iv) Coulomb interaction plus the SU(8) optical potential, but with $\alpha = 1.2$ or without a nucleon gap (Table 4 with results only for ^{12}C).
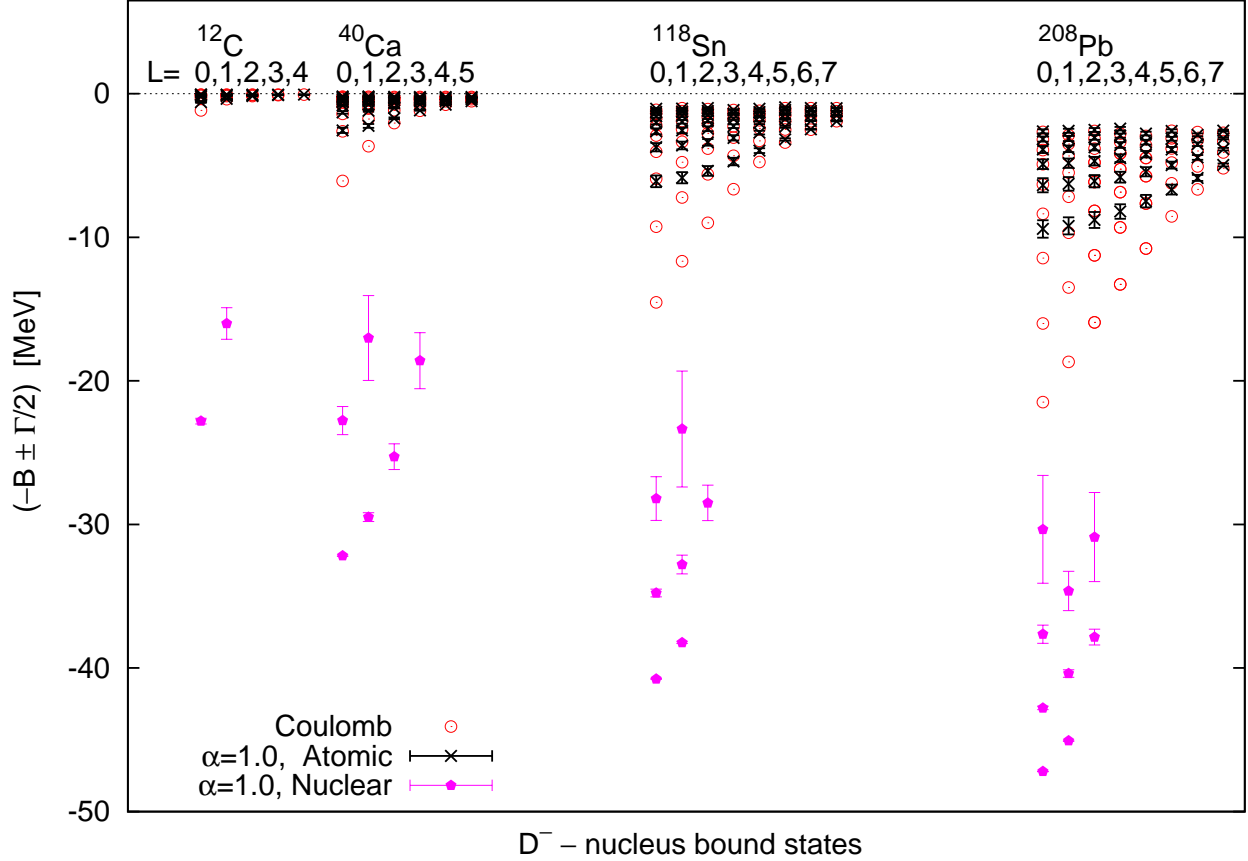
Figure 3: Same as in Fig. 2, but including states of nuclear type (pentagons) as well. In this case no scale factor has been applied.

v) Coulomb interaction plus the SU(4) optical potential of Ref. [23], where the $\bar{D}^*N$ coupled-channel effects are ignored (Table 5).

The calculation that we deem more realistic for D^- states is that obtained by using the SU(8) model with $\alpha = 1$ and with a nucleon extraction energy (gap) of 8 MeV. The predicted spectrum of low-lying states is given in Table 2 and displayed in Figs. 2 and 3. In these figures, the pure Coulomb levels are also shown for comparison. A salient feature of the spectrum is the presence of two types of states: atomic and nuclear ones.

The states of atomic type follow from distortion of the pure Coulombian levels, they have moderate widths and they exist for all angular momenta. For these states, the nuclear interaction is a perturbation and their wave functions have support mainly outside of the nucleus. As compared to the Coulombian levels, the states of atomic type are shifted upwards, i.e., they are less bound. So effectively, they feel a repulsive interaction. The atomic states are only sensible to the region of small densities and small energies, and in this region the potential can be repulsive. (To interpret correctly the optical potential profile in Fig. 1, it should be taken into account that, by minimal coupling, the energy argument of optical potential is not q^0 but q^0 increased by the local Coulomb potential.) Part of the repulsion comes also from the imaginary part of the optical potential,

a well known effect in exotic atoms [42]. In addition, the existence of states of nuclear type should tend to push upwards the atomic states. Yet, for heavier nuclei, some spurious repulsion could be introduced by our simplifying approximation of using symmetric nuclear matter in the calculation of the optical potential[4]. As expected, strong interaction shifts and widths become much larger for low angular momenta and heavier nuclei. Roughly, the nuclear interaction turns out to be significant for $L \leq 1, 2, 5$, and 6 for ^{12}C, ^{40}Ca, ^{112}Sn and ^{208}Pb, respectively. Likewise, the (strong) widths and shifts are larger for states with lower quantum numbers due to a greater overlap of the wave function with the nucleus. (Of course, the electromagnetic width, not included, increases with the quantum number instead.)

On the other hand, the spectrum of the states of nuclear type lies below, and well separated from, that of the atomic states and also from the Coulombian levels. The gap between nuclear and atomic states ranges for 15 to 20 MeV for all nuclei, whereas the gap with the Coulomb states decreases with the nuclear size. The nuclear states have widths ranging from few keV to several MeV and have considerable binding energies of tenths of MeV, pointing out to a sizable overlap of their wave function with the nucleus. The states of nuclear type exist only for the lower angular momenta and there is only a finite number of them that increases with the nuclear mass. We should note that, being the optical potential complex and energy dependent, the usual theorems of classification of states by nodes do not apply, and so it is much harder to guarantee that all levels in a given region of the complex energy plane have been found.[5] An interesting feature of the nuclear states is that their widths decrease as the binding energies increase. (This is opposite to what happens to atomic states regarding their strong width.) The profile of widths as a function of the energy of the states just mimics the profile of the imaginary part of the optical potential (see Fig. 1). The lowest states have small widths as they fall in the tail of the imaginary part of the optical potential. The low lying states are already inside the nucleus, so the overlap does not increase by lowering the energy, and instead they have less phase-space available for decay. This also explains why the widths of the nuclear states decrease with the size of the nucleus: for larger nuclei the ground state tends to be closer to the bottom of the potential, and hence the available kinetic energy to knockout nucleons decreases.

In Table 2 we also quote results from Ref. [10] obtained in ^{208}Pb within a quark-meson coupling model [11]. Widths were disregarded in [10]. The numbers quoted for their model $\tilde{V}^q_\omega$ turn out to be not very different from ours for atomic states. Besides, one would be tempted to say that the $1s$, $2s$ and $1p$ levels of the model V^q_ω of Ref. [10] match our $3s$, $4s$, and $3p$ levels of nuclear type.

In Table 3 and Fig. 4 we show the spectrum of $\bar{D}^0$-nucleus bound states. This spectrum approximately matches that of the D^--states of the nuclear type. The $1p$ levels of the two heavier nuclei are missing in the $\bar{D}^0$ spectrum. The most likely scenario is that those states exist but we have been unable to pin them down due to numerical instabilities. The $\bar{D}^0$ and D^- binding energies show a systematic difference, which can be traced back to the missing Coulomb attraction in the $\bar{D}^0$ case. The widths are also comparable but systematically larger in the charged case. This can be easily understood since in presence of the Coulomb attraction, the binding energies are larger, which forces the D^--states to explore/be sensitive to higher nuclear densities. In the

---

[4] Attending to the in vacuum $\bar{D}N$ T-matrix, since $(T^{(I=1,J=1/2)} - T^{(I=0,J=1/2)})(\rho_n - \rho_p)$ is negative near threshold, the asymmetry effect is expected to be attractive for heavier nuclei richer in neutrons than in protons.

[5] We do not include some very wide states that overlap with the continuum. The fact that these states are very rare makes more appropriate our approximation of using only the real part of the energy as argument of the $\bar{D}$ optical potential in the Schrödinger equation.
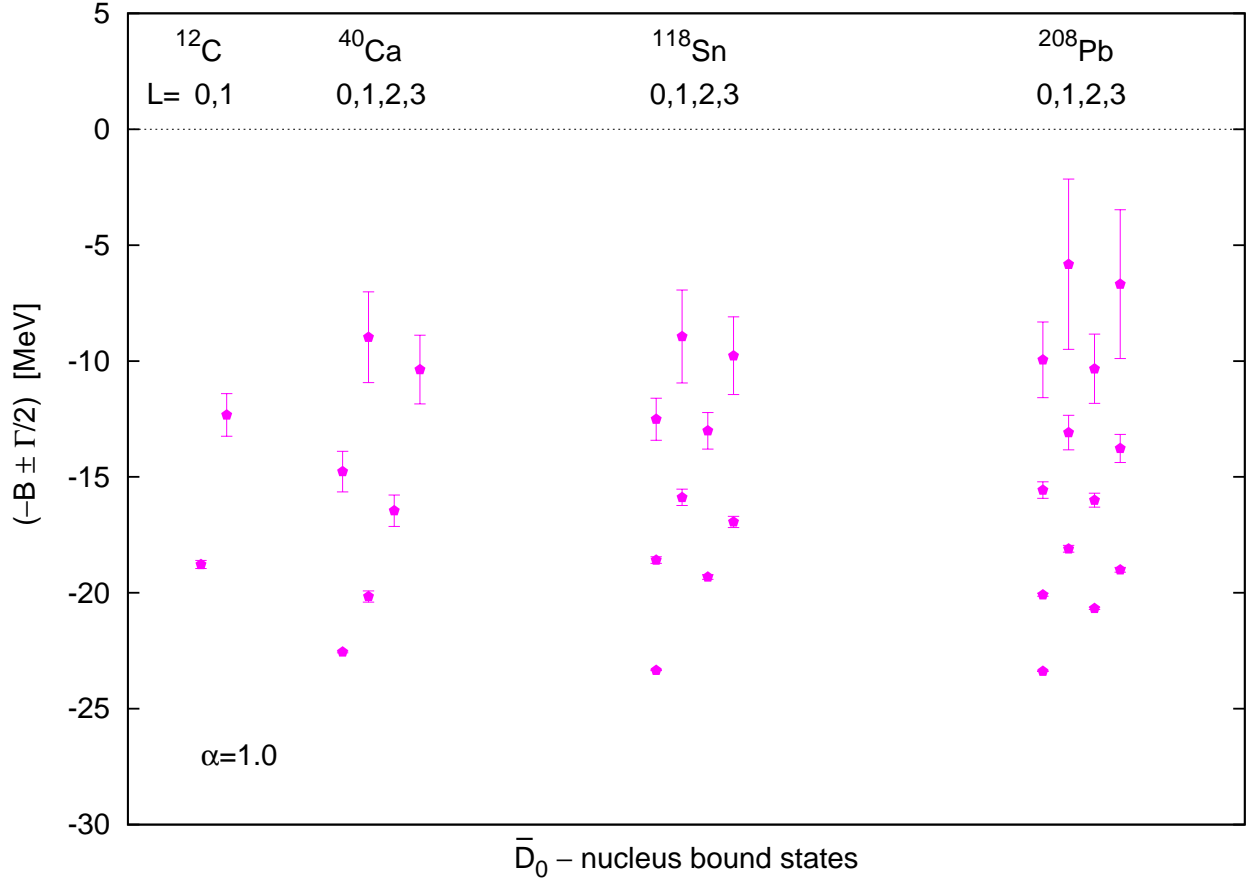
Figure 4: $\bar{D}^0$ nuclear levels, for different nuclei and angular momenta predicted by the SU(8) model derived in this work (see Fig. 1), with $\alpha = 1$ and gap $8\,\mathrm{MeV}$ (Table 3).

same table we also compare with the V_ω^q model predictions of Ref. [10] for lead. (The model $\tilde{V}_\omega^q$ does not produce bound states.) We find an excellent agreement with these results for the $1s$ and $2s$ levels.

Next, we try to better understand some systematic effects that affect to our predictions. First, we have considered the dependence of our results on the choice of the subtraction point used to renormalize the ultraviolet divergent loop functions. Thus, we have re-calculated binding energies and widths, of both atomic and nuclear levels, with $\alpha = 1.2$. These new results are collected in Table 4 for carbon and can be compared with those of Table 2 obtained with $\alpha = 1.0$. From the behaviour exhibited in Fig. 1, one might expect moderate changes, that would lead, in general, to smaller widths and binding energies when α is set to 1.2. However, the computed $\alpha = 1.2$ levels (see Table 4) do not always follow this pattern. The observed deviations are probably induced by the strong energy dependence of the optical potential. Though changes are very small for atomic states with $L > 0$, they become much larger for the $L = 0$ levels and also for the spectrum of nuclear states. A similar calculation for heavier nuclei shows that the effect is smaller, but the number of nuclear states changes occasionally. This might be a true qualitative change in the spectrum induced by the differences in the potentials. However, it could be just due to the fact

that some nuclear states have been missed in the difficult search throughout the complex plane. For the $\bar{D}^0$ levels, the effect of changing α from 1 to 1.2 is completely similar to that already noted for the states of nuclear type in the charged case, that is, less binding and smaller widths, and occasionally, a change in the number of levels. In the case of the $(C = +1, S = 0)$ sector, the subtraction point α could be fixed in the free space by tuning the pole position of the three star $\Lambda_c(2595)$ and $\Lambda_c(2625)$ resonances (see for instance [20]). Thus in contrast with the situation here, our previous study [32] on the possible existence of D^0-nuclear bound states was free, to a large extent, of this source of theoretical uncertainties. The lack of experimental information on the $C = -1$ sector, however, prevents us to fix more precisely the subtraction point used in the renormalization scheme proposed in [29] and employed in the free space calculation of Ref. [21], in which the results of this work are based[6]. Thus, we should take the differences between the results displayed in Tables 2 and 4 as a hint on the nature of the theoretical uncertainties that affect to our results. Other sources of uncertainties will be discussed below, but among all of them, those related to the choice of the subtraction point are certainly the largest ones.

For instance, in the calculation we have also included in an approximated way the effect of the existence of a non-zero gap in the nucleon spectrum, separating nucleons in the Fermi sea from the free ones. In Table 4 we show the results without gap for ^{12}C. The gap reduces the width of the states of nuclear type, but however their binding energies are not much affected. On the other hand, the changes in atomic states are also small. With regard to the SU(4) model, which ignores $\bar{D}^*N$ coupled channel effects, we observe a repulsive interaction for the $\bar{D}$ in nuclear matter. As a consequence the corresponding optical potential is repulsive and purely real in the region of interest. This model predicts D^- atoms stable under strong interactions with levels of atomic type uniformly moved upwards in energy as compared to the pure Coulombian prediction (see Table 5). The repulsion is smaller than for SU(8), presumably due to the lack of imaginary part. However, we believe the results of Table 2 are more realistic than any of those commented above, because neither neglecting the finite nucleon extraction energy, nor ignoring the HQSS constraints/requirements are approximations physically acceptable.

4 D^- atom decay modes

As noted in the Introduction, D^- atoms[7] stand out among other exotic atoms. This is also true regarding their decay modes. Two mechanisms are available for decay, namely, particle-hole production, $\bar{D} \to \bar{D}NN^{-1}$, and pentaquark production, $\bar{D} \to X(2805)N^{-1}$.

Let us disregard pentaquark production momentarily. A particle-hole production mechanism is of course present in other exotic atoms. However, in other atoms this is not the dominant decay: In pionic atoms the non electromagnetic width comes from absorption of the pion by two or more nucleons. In η-nucleus systems the η carries no charge and it can be easily absorbed into particle-hole excitations or else, it can be traded by the much lighter pion. In $\bar{K}$-atoms the K^- carries strangeness and so it cannot just be absorbed into particle-hole excitations, but the

---

[6]For instance, note that for $\alpha = 1$, there exists a prominent delta-like structure in the in-medium amplitudes, at very low densities, due to the $X(2805)$ exotic bound state. However, it is clearly smeared out when α is set to 1.2, since the $X(2805)$ baryon pentaquark is not longer bound for this value of α, and it becomes then a more or less narrow resonance.

[7]Throughout this discussion, "D^- atoms" refer to all $\bar{D}$-nucleus bound states, whether they are of atomic or of nuclear type.

s quark can be passed to a baryon. There is energy available for processes with mesons in the final state, $\bar{K} \to \pi\Lambda N^{-1}$ and $\pi\Sigma N^{-1}$, or without them, $\bar{K} \to N\Lambda N^{-1}N^{-1}$ and $N\Sigma N^{-1}N^{-1}$ [43]. Likewise, in D^0-nucleus systems mesonic mechanisms, $D^0 \to \pi\Lambda_c N^{-1}$ and $D^0 \to \pi\Sigma_c N^{-1}$, and non mesonic ones, $D^0 \to N\Lambda_c N^{-1}N^{-1}$ and $D^0 \to N\Sigma_c N^{-1}N^{-1}$, are energetically allowed. In those decay modes, the c quark is transferred to a baryon.

In this regard, the situation of the D^- atoms is qualitatively different from all the previous ones. Of course, the D^- cannot just be absorbed into particle-hole excitations, as was the case of pion or η. Also, it cannot combine with a nucleon to decay to a lighter meson-baryon channel, as happens for K^- or D^0, because baryons cannot carry the negative charm of the $\bar{D}$ and there are no lighter charmed mesons. Put in another way, clusters like $\bar{D}N$ or $\bar{D}NN$ are stable under strong decay as there are no lighter hadronic states with same charm and baryonic quantum numbers. (Recall that the possibility of pentaquark formation is not being considered yet.)

These remarks would also apply to an hypothetic K-nucleus bound state. However such system does not exist since the KN interaction is repulsive, as it is Coulomb for the K^+. On the contrary the D^- will form of necessity a bound state with the nucleus, if by no other mechanism, through Coulomb interaction. (Even if the strong interaction were repulsive it would vanish outside the nucleus and the atom would be formed anyway.) So D^- atoms are truly special: other exotic atoms decay through *hadronic* mechanisms (to lighter hadronic states) while D^- atoms can only decay through *many-body* mechanisms, e.g., $\bar{D}N \to \bar{D}N$, where the $\bar{D}$ falls to a lower level transferring energy to the nucleus.

The fact that particle-hole production is the dominant mechanism for decay has important consequences for D^- atoms, both phenomenological and theoretical. Consider for instance the ground state of a K^- atom. Although it is the lowest atomic state, nothing prevents it from decaying to lighter hadronic states (transferring the s quark to a baryon as discussed above). On the other hand, for the *ground state* of a D^- atom no such lighter hadronic state exists, so one should expect no width in this case. Put in another way, the $\bar{D}$ cannot go to a lower atomic state to be able to eject a nucleon. To be precise, for the final state we should actually consider, not the spectrum of the original atom but that of the daughter nucleus (with one less nucleon). The difference between the two spectra is not expected to be large, at least for not very small nuclei, and moreover, we expect the ground state of the daughter-nucleus atom to be less bound, reinforcing the argument. In this view, the fate of the D^- atom would be to form a stable $\bar{D}$-nucleus bound state, which would eventually decay through weak interaction.

From the theoretical side, the ground state argument just presented shows that the widths, as predicted by a naive application of the $\bar{D}$ optical potential, tend to be overestimated for low lying states. The LDA replaces the true discrete spectrum of the $\bar{D}$ (in the daughter nucleus) by a continuum of states starting from the bottom of the optical potential upwards. As the energy of the ground state will be above that bottom, the LDA incorrectly assigns available phase space for particle-hole decay. Of course, the same mechanism of *spectral blocking* is present in the application of the LDA to the study of other exotic atoms but this is not so crucial there because the decay is dominated by other mechanisms which give sizable width even to the ground state.

Another effect has to be considered as well, namely, the existence of a gap in the spectrum of nucleons, separating nucleons in the Fermi sea from the free ones (or from excited states, beyond the LDA). The *gap blocking* tends to quench the widths from particle-hole production, as the nucleons need a minimum energy to escape the nucleus, and so it helps to reduce or even remove the width of low lying D^- atom states. We have included such an effect in an approximated way,

just by reducing the energy argument in the imaginary part of the optical potential by a constant amount of $8\,\text{MeV}$.[8]

Up to now we have disregarded the pentaquark production mechanism. The $X(2805)$ in the vacuum scheme of Ref. [21] is a bound state of N and $\bar{D}$. The binding energy is quite small, about $1.4\,\text{MeV}$, so this pole is very close to the $\bar{D}N$ threshold. A key issue is whether this state remains bound or moves to a resonance at finite nuclear density. When Pauli blocking is enforced, the threshold moves upwards, favoring the bound state over the resonance. The situation changes completely when the $\bar{D}$ optical potential is also taken into account by means of the self-consistent procedure. In the region of interest, the effect of the $\bar{D}$ optical potential turns out to be attractive. This brings the threshold downwards. In addition, the pole in medium moves to higher energies. The net result is that, even for a density as small as $0.1\,\rho_0$ (the lowest density accessible by our calculation), the pole lies above the threshold and turns into a resonance. For this density and higher, the pentaquark would decay into N and $\bar{D}$, and this brings us back to the particle-hole decay mechanism. Nevertheless, note that, by continuity, there should be a critical density below which the pole is below threshold, and so allowing the pentaquark production mechanism. Thus this mechanism always has some contribution, however small, to the width (even for the ground state). The situation may also change due to gap blocking and spectral blocking, which tend to push the threshold upwards, thereby favoring the pentaquark production mechanism.

The presence of a pole in the T-matrix in the region of interest makes the technical problem rather difficult. This has forced us to extrapolate the optical potential from $\rho = 0.1\,\rho_0$ to lower densities when needed, without spectral blocking and with approximate gap blocking. This results in treating the pole always as a resonance in our calculation. So, even for the ground state, our calculation nominally attributes all widths to particle-hole production. A more detailed treatment would provide pentaquark production as well, below a certain critical density. In fact, for the ground state this would be the only decay mode. Although nominally the widths we find come from particle-hole, for low lying states there should be a genuine contribution coming from the pole albeit distorted by the coupling to particle-hole. This suggests that the width computed for the ground state is a rough estimate of the true width from pentaquark production to be obtained in a more complete treatment without spurious particle-hole decay in the ground state.

Phenomenologically, it is important to note that the in-medium $X(2805)$ state is produced by a bound N and a bound $\bar{D}$. Because the pentaquark formation energy is so small, the kinetic energy released is also small and the pentaquark remains bound in the nucleus after formation. This suggests that after the electromagnetic cascade in the atomic levels and the subsequent particle-hole emission cascade in the nuclear levels, the fate of the D^- atom could be a pentaquark-nucleus bound state. This would be stable until weak decay of the $\bar{D}$ meson. Of course this is a fascinating possibility both theoretically and experimentally.

The approximate implementation of the gap blocking and the lack of spectral blocking suggest that the actual widths will be somewhat smaller that those obtained here. A side effect of a smaller imaginary part would be an effective increase in the binding of the states.

---

[8]A more correct procedure would be to shift only the energy of the hole line in Eqs. (8) and (9), i.e., $E_N(\boldsymbol{p}) \to E_N(\boldsymbol{p}) - E_{\text{gap}}$, but this turns out to be technically involved due to the presence of the $X(2805)$ state. This is a pole in the T-matrix which turns from a bound state to a resonance as the nuclear density increases.

5 Summary and conclusions

A self-consistent calculation of the $\bar{D}$ self-energy has been carried out in symmetric nuclear matter using unitarized coupled-channel theory. The model is based on SU(8) spin-flavor symmetry and enjoys heavy quark spin symmetry. Two renormalization prescriptions have been used in order to estimate the systematic error involved. We find that the presence of a bound state near the $\bar{D}N$ threshold makes the optical potential to be strongly energy and density dependent. In contrast with SU(4) based models, the optical potential is mostly attractive (except for a repulsive region for low densities near threshold, relevant for levels of atomic type) and develops an imaginary part to particle-hole production and possibly to pentaquark production inside the nucleus. Unlike other hadronic atoms, no other relevant decay mechanisms exist for the $\bar{D}$ in nuclear matter around threshold.

Using the local density approximation, we have computed the levels and widths for low lying states of several nuclei, light and heavy. The results are summarized in Figs. 2 and 3 for D^--atoms and in Fig. 4 for $\bar{D}^0$-nucleus bound states. The spectrum presents two types of states, atomic and nuclear, for all studied nuclei[9]. The nuclear states exists for lower angular momenta only. As compared to the pure Coulomb levels, the atomic states are less bound and the nuclear ones are more bound and may present a sizable width.

A number of approximations have been necessary in an already highly sophisticated calculation to render it feasible. Nevertheless, this is the first systematic study of D^- atoms that accounts properly for HQSS and for the many-body mechanisms responsible for the widths of the states. We can draw two general conclusions from the present work. First, that in the study of nuclear systems involving charm, it is important to use a model fulfilling the QCD requirement of heavy quark spin symmetry. The vector-meson partner of the $\bar{D}$, the $\bar{D}^*$, has a similar mass and hence its inclusion substantially modifies the $\bar{D}N$ dynamics producing a non trivial structure in its T-matrix near threshold. And second, the anti-quark c in the $\bar{D}$ cannot be transferred to the baryons, and in particular, a $\bar{D}N$ pair has no open channels to decay. For this reason it has been often assumed that the $\bar{D}$ would not interact much with the nucleus and could be treated as an spectator. We find that this is not the case, and in fact a rich spectrum is obtained with sizable shifts and widths in the states.

The observation of the states predicted here might be feasible in the PANDA and CBM experiments at the future FAIR facility at Darmstadt, and it would certainly shed light to unravel the fascinating $\bar{D}N$ dynamics, both in the free space and when the pair is embedded in a dense nuclear medium.

---

[9]Of course, atomic like states do not appear in the $\bar{D}^0$ case.

within the framework of the LOEWE program by the State of Hesse (Germany).

References

[1] M. Ericson and T. E. O. Ericson, Annals Phys. **36**, 323 (1966).

[2] E. Friedman and A. Gal, Phys.Rept. **452**, 89 (2007), [0705.3965].

[3] J. Nieves, E. Oset and C. García-Recio, Nucl. Phys. **A554**, 509 (1993).

[4] C. Garcia-Recio, J. Nieves and E. Oset, Nucl.Phys. **A547**, 473 (1992).

[5] S. Hirenzaki, Mod.Phys.Lett. **A23**, 2497 (2008).

[6] H. Gilg *et al.*, Phys.Rev. **C62**, 025201 (2000).

[7] S. Wycech *et al.*, Phys.Rev. **C76**, 034316 (2007), [nucl-th/0702029].

[8] B. Klos *et al.*, Phys.Rev. **C76**, 014311 (2007), [nucl-ex/0702016].

[9] A. Trzcinska *et al.*, Phys.Rev.Lett. **87**, 082501 (2001).

[10] K. Tsushima, D.-H. Lu, A. W. Thomas, K. Saito and R. Landau, Phys.Rev. **C59**, 2824 (1999), [nucl-th/9810016].

[11] P. A. Guichon, Phys.Lett. **B200**, 235 (1988).

[12] S. Yasui and K. Sudoh, Phys.Rev. **D80**, 034008 (2009), [0906.1452].

[13] U. Wiedner, Prog.Part.Nucl.Phys. **66**, 477 (2011), [1104.3961].

[14] Physics Performance Report for PANDA: Strong Interaction Studies with Antiprotons, PANDA Collaboration, arXiv:0903.3905 [http://www.gsi.de/PANDA].

[15] J. Aichelin et al., The CBM Physics Book, Lect. Notes in Phys. **814** (2011) 1-960, eds. B. Friman, C. Hohne, J. Knoll, S. Leupold, J. Randrup, R. Rapp and P. Senger (Springer)

[16] CBM Collaboration, P. Staszel, Acta Phys.Polon. **B41**, 341 (2010).

[17] http://www.gsi.de/fair/.

[18] N. Isgur and M. B. Wise, Phys. Lett. **B232**, 113 (1989).

[19] M. Neubert, Phys. Rept. **245**, 259 (1994), [hep-ph/9306320].

[20] C. García-Recio *et al.*, Phys. Rev. **D79**, 054004 (2009), [0807.2969].

[21] D. Gamermann, C. Garcia-Recio, J. Nieves, L. Salcedo and L. Tolos, Phys.Rev. **D81**, 094016 (2010), [1002.2763].

[22] M. Lutz and C. Korpa, Phys.Lett. **B633**, 43 (2006), [nucl-th/0510006].

[23] L. Tolos, A. Ramos and T. Mizutani, Phys.Rev. **C77**, 015207 (2008), [0710.2684].

[24] C. Jimenez-Tejero, A. Ramos, L. Tolos and I. Vidana, Phys.Rev. **C84**, 015208 (2011), [1102.4786].

[25] L. Tolos, C. Garcia-Recio and J. Nieves, Phys.Rev. **C80**, 065202 (2009), [0905.4859].

[26] C. Garcia-Recio, J. Nieves and L. Salcedo, Phys.Rev. **D74**, 036004 (2006), [hep-ph/0605059].

[27] C. García-Recio, J. Nieves and L. L. Salcedo, Phys. Rev. **D74**, 034025 (2006), [hep-ph/0505233].

[28] C. Garcia-Recio and L. Salcedo, J.Math.Phys. **52**, 043503 (2011), [1010.5667].

[29] J. Hofmann and M. Lutz, Nucl.Phys. **A763**, 90 (2005), [hep-ph/0507071].

[30] L. Tolos, R. Molina, E. Oset and A. Ramos, Phys.Rev. **C82**, 045210 (2010), [1006.3454].

[31] C. Garcia-Recio, J. Nieves, T. Inoue and E. Oset, Phys.Lett. **B550**, 47 (2002), [nucl-th/0206024].

[32] C. Garcia-Recio, J. Nieves and L. Tolos, Phys.Lett. **B690**, 369 (2010), [1004.2634].

[33] E. Oset and L. Salcedo, J.Comput.Phys. **57**, 361 (1985).

[34] C. Garcia-Recio, E. Oset, L. Salcedo, D. Strottman and M. Lopez, Nucl.Phys. **A526**, 685 (1991).

[35] A. Baca, C. Garcia-Recio and J. Nieves, Nucl.Phys. **A673**, 335 (2000), [nucl-th/0001060].

[36] J. Yamagata, H. Nagahiro, Y. Okumura and S. Hirenzaki, Prog.Theor.Phys. **114**, 301 (2005), [nucl-th/0503039].

[37] J. Yamagata-Sekihara, D. Cabrera, M. J. Vicente Vacas and S. Hirenzaki, Prog.Theor.Phys. **124**, 147 (2010), [1001.2235].

[38] C. De Jager, H. De Vries and C. De Vries, Atom.Data Nucl.Data Tabl. **14**, 479 (1974).

[39] H. De Vries, C. De Jager and C. De Vries, Atom.Data Nucl.Data Tabl. **36**, 495 (1987).

[40] J. W. Negele and D. Vautherin, Phys.Rev. **C11**, 1031 (1975).

[41] L. Salcedo, E. Oset, M. Vicente-Vacas and C. Garcia-Recio, Nucl.Phys. **A484**, 557 (1988).

[42] M. Krell, Phys.Rev.Lett. **26**, 584 (1971).

[43] A. Ramos and E. Oset, Nucl. Phys. **A671**, 481 (2000), [nucl-th/9906016].

Table 1: D^--atom binding energies B [keV], calculated using only the Coulomb potential for several nuclei and orbital angular momenta (L). The Coulomb degeneracy is corrected by nuclear finite size and vacuum polarization effects.

L	^{12}C				
0	1158	333	155	89	58
1	384	171	96	61	
2	171	96	62		
3	96	62			
4	62				

L	^{40}Ca							
0	6073	2626	1412	875	594	429	324	254	204
1	3664	1768	1038	682	482	359	277	220	
2	2052	1156	742	517	381	292	231		
3	1190	760	528	388	297	234			
4	762	529	388	297	235				
5	529	388	297	235					

L	^{118}Sn							
0	14536	9260	5919	4038	2912	2194	1710	1369	1121
1	11665	7230	4766	3349	2475	1901	1505	1220	
2	8996	5611	3821	2764	2091	1637	1315		
3	6650	4321	3051	2272	1758	1401			
4	4760	3290	2429	1855	1469				
5	3404	2494	1907	1506					
6	2509	1920	1516						
7	1920	1517							

L	^{208}Pb							
0	21485	16006	11454	8371	6317	4915	3923	3200	2658
1	18680	13502	9682	7180	5503	4341	3506	2888	
2	15929	11256	8167	6151	4787	3825	3124	2599	
3	13276	9310	6863	5258	4154	3362	2777		
4	10787	7654	5749	4482	3595	2948			
5	8550	6249	4801	3813	3104	2578			
6	6662	5063	3991	3232	2672				
7	5190	4089	3306	2729					

Table 2: Complex D^--atom energies $(B, \Gamma/2)$ for several nuclei. The calculation includes Coulomb potential plus the SU(8) energy dependent optical potential with $\alpha = 1$ and a nucleon gap of 8 MeV (see Fig. 1). To preserve the structure of the atomic states, the states of nuclear type (when there exist) are displayed in the first line that corresponds to each of the angular momentum entries. The second line in the entry contains the energies of the atomic states. Results of Ref. [10] for the binding energies in ^{208}Pb are also shown for model $\tilde{V}_\omega^q$ between square brackets and for model V_ω^q without brackets.

^{12}C, $\alpha = 1.0$, gap $= 8\,$MeV

L	$(B, \Gamma/2)$ [keV]			
0	(22800, 199)			
	(585, 51)	(222, 12)	(116, 5)	(71, 2)
1	(16000, 1100)			
	(353, 9)	(160, 3)	(91, 1)	(59, 1)
2	(171, 0.1)	(96, 0.1)	(62, 0.0)	
3	(96, 0)	(62, 0)		
4	(62, 0)			

^{40}Ca, $\alpha = 1.0$, gap $= 8\,$MeV

L	$(B, \Gamma/2)$ [keV]							
0	(32177, 48)	(22764, 978)						
	(2556, 184)	(1305, 85)	(806, 45)	(550, 27)	(400, 17)	(304, 12)	(239, 8)	(193, 6)
1	(29486, 306)	(17022, 2956)						
	(2244, 138)	(1187, 66)	(748, 36)	(517, 22)	(379, 14)	(291, 10)	(230, 7)	(186, 5)
2	(25282, 892)							
	(1716, 67)	(981, 36)	(643, 21)	(456, 13)	(341, 9)	(264, 6)	(211, 5)	(172, 3)
3	(18596, 1952)							
	(1160, 13)	(738, 10)	(512, 7)	(377, 5)	(289, 3)	(229, 2)	(185, 2)	
4	(761, 1)	(528, 1)	(388, 1)	(297, 0)	(234, 0)	(190, 0)		
5	(528, 0)	(388, 0)	(297, 0)	(235, 0)	(190, 0)			

^{118}Sn, $\alpha = 1.0$, gap $= 8\,$MeV

L	$(B, \Gamma/2)$ [keV]							
0	(40768, 25)	(35777, 271)	(28200, 1527)					
	(6102, 414)	(3727, 286)	(2619, 206)	(2004, 134)	(1576, 92)	(1272, 67)	(1048, 51)	(878, 39)
1	(38227, 69)	(32794, 651)	(23353, 4033)					
	(5853, 389)	(3612, 268)	(2558, 192)	(1960, 125)	(1544, 87)	(1248, 64)	(1030, 48)	(864, 37)
2	(28504, 1236)							
	(5378, 337)	(3390, 234)	(2439, 165)	(1873, 109)	(1481, 77)	(1201, 57)	(994, 43)	(836, 33)
3	(4726, 260)	(3081, 187)	(2262, 129)	(1747, 88)	(1390, 63)	(1134, 47)	(943, 36)	(796, 28)
4	(3968, 168)	(2709, 130)	(2033, 89)	(1587, 63)	(1275, 46)	(1048, 35)	(877, 27)	(745, 21)
5	(3189, 80)	(2308, 68)	(1769, 50)	(1403, 37)	(1141, 28)	(947, 22)	(799, 17)	
6	(2482, 20)	(1889, 21)	(1489, 18)	(1205, 15)	(995, 12)	(836, 10)		
7	(1919, 2)	(1515, 2)	(1226, 3)	(1013, 2)	(850, 2)			

^{208}Pb, $\alpha = 1.0$, gap $= 8\,$MeV — **^{208}Pb, Ref. [10]**

L	$(B, \ \Gamma/2)$ [keV]						B [keV]	
0	(47203, 21)	(42781, 121)	(37644, 636)	(30343, 3755)			35.2×10^3	30×10^3
	(9418, 606)	(6375, 496)	(4912, 334)	(3892, 243)	(3160, 184)	(2618, 142)	$[10.6 \times 10^3]$	$[7.7 \times 10^3]$
1	(45065, 45)	(40385, 265)	(34634, 1370)				32.1×10^3	
	(9206, 590)	(6283, 474)	(4841, 322)	(3839, 235)	(3120, 178)	(2587, 138)	$[10.2 \times 10^3]$	
2	(37845, 545)	(30879, 3098)						
	(8793, 557)	(6096, 434)	(4700, 299)	(3734, 219)	(3040, 167)	(2526, 130)		
3	(8204, 504)	(5813, 379)	(4491, 266)	(3579, 197)	(2924, 150)	(2436, 117)		
4	(7480, 434)	(5437, 314)	(4219, 225)	(3379, 168)	(2773, 129)	(2319, 102)		
5	(6676, 344)	(4977, 242)	(3891, 177)	(3139, 135)	(2592, 105)	(2180, 94)		

Table 3: Binding energy and half-widths, $(B, \Gamma/2)$, in keV, of $\bar{D}^0$-nucleus levels for ^{12}C, ^{40}Ca, ^{112}Sn and ^{208}Pb and several angular momenta. The bound levels have been obtained with the SU(8) energy dependent optical potential of Fig. 1 with $\alpha = 1$ and a nucleon gap of 8 MeV. Results of Ref. [10] for ^{208}Pb are also shown for the model V_ω^q (the model $\tilde{V}_\omega^q$ does not give rise to any bound states).

^{12}C, $\bar{D}^0$, $\alpha = 1.0$, gap $= 8$ MeV	
L	$(B, \Gamma/2)$ [keV]
0	$(18779, 176)$
1	$(12324, 918)$

^{40}Ca, $\bar{D}^0$, $\alpha = 1.0$, gap $= 8$ MeV		
L	$(B, \Gamma/2)$ [keV]	
0	$(22549, 38)$	$(14769, 874)$
1	$(20158, 241)$	$(8971, 1957)$
2	$(16457, 679)$	
3	$(10370, 1480)$	

^{118}Sn, $\bar{D}^0$, $\alpha = 1.0$, gap $= 8$ MeV		
L	$(B, \Gamma/2)$ [keV]	
0	$(23339, 17)$	$(18590, 143)$	$(12510, 907)$
1		$(15882, 355)$	$(8939, 2004)$
2	$(19317, 106)$	$(13009, 787)$	
3	$(16941, 241)$	$(9770, 1677)$	

^{208}Pb, $\bar{D}^0$, $\alpha = 1.0$, gap $= 8$ MeV				^{208}Pb, Ref. [10]	
L	$(B, \Gamma/2)$ [keV]			B [keV]	
0	$(23381, 13)$	$(20085, 66)$	$(15569, 358)$	$(9951, 1633)$	25.4×10^3 19.7×10^3
1		$(18102, 146)$	$(13086, 747)$	$(5823, 3675)$	23.1×10^3
2	$(20671, 50)$	$(16002, 304)$	$(10336, 1494)$		
3	$(19006, 100)$	$(13770, 608)$	$(6682, 3208)$		

20

Table 4: Same as in Table 2, but only for ^{12}C and different combinations of α and the nucleon gap.

L	^{12}C, $\quad \alpha = 1.2, \quad$ gap $= 8\,\mathrm{MeV}$			
	$(B, \Gamma/2)$ [keV]			
0	$(16300, 104)$	$(1829, 949)$		
	$(373, 90)$	$(167, 28)$	$(94, 12)$	$(61, 6)$
1	$(9300, 595)$			
	$(354, 11)$	$(160, 4)$	$(91, 2)$	$(59, 1)$
2	$(171, 1)$	$(96, 0.6)$	$(62, 0.3)$	
3	$(96, 0)$	$(62, 0)$		
4	$(62, 0)$			

L	^{12}C, $\quad \alpha = 1.0, \quad$ gap $= 0\,\mathrm{MeV}$			
	$(B, \Gamma/2)$ [keV]			
0	$(22700, 2100)$			
	$(555, 47)$	$(215, 12)$	$(113, 5)$	$(70, 2)$
1	$(15700, 6900)$			
	$(348, 11)$	$(158, 4)$	$(91, 2)$	$(59, 1)$
2	$(171, 0.2)$	$(96, 0.1)$	$(62, 0.1)$	
3	$(96, 0)$	$(62, 0)$		
4	$(62, 0)$			

Table 5: D^--atom binding energies B in keV, calculated using the SU(4) optical potential of Ref. [23] together with the Coulomb interaction.

L	^{12}C			
0	666	241	123	75
1	364	164	93	
2	171	96		
3	96			

L	^{40}Ca				
0	2946	1487	903	607	436
1	2505	1315	818	559	407
2	1816	1038	677	477	
3	1173	748	519		
4	762	528			
5	529				

L	^{118}Sn						
0	7024	4442	3106	2303	1778	1415	1153
1	6692	4255	2988	2224	1722	1374	1122
2	6068	3911	2775	2082	1623	1302	1069
3	5219	3453	2493	1895	1492	1207	
4	4250	2929	2168	1677	1338		
5	3295	2394	1828	1444			
6	2498	1905	1502				
7	1920	1516					

L	^{208}Pb								
0	10787	7503	5662	4612	4060	3404	2826	2374	2021
1	10520	7318	5491	4305	3481	2881	2430	2080	
2	10002	6980	5246	4113	3320	2740	2302		
3	9261	6513	4922	3876	3140	2600	2190		
4	8333	5943	4535	3598	2933	2440	2064		
5	7272	5301	4101	3287	2701	2263			
6	6146	4619	3640	2955	2453	2072			
7	5051	3937	3170	2614	2196				